Anti-adhesive bioactive glasses via oligosiloxane deposition and plasma treatment

Surfaces and Interfaces 83 (2026) 108515

Contents lists available at ScienceDirect

Surfaces and Interfaces

journal homepage: www.sciencedirect.com/journal/surfaces-and-interfaces

Anti-adhesive bioactive glasses via oligosiloxane deposition and plasma treatment

Kevin Pontillo [a], Martina Masserano [a], Ziba Najmi [c], Andrea Cochis [c], Lia Rimondini [c], Sara Ferraris [a,b], Katiuscia Costabello [d], Manuel Lai [d], Enrica Vernè [a,b], Marta Miola [a,b,*]

[a] Department of Applied Science and Technology, Politecnico di Torino, Institute of Materials Engineering and Physics, Corso Duca degli Abruzzi, 24, 10129 Torino, Italy
[b] PolitoBioMED Lab, Politecnico di Torino, Corso Castelfidardo, 30A, 10129 Torino, Italy
[c] Department of Health Sciences, Center for Translational Research on Autoimmune and Allergic Disease—CAAD, Università Del Piemonte Orientale (UPO), 28100 Novara, Italy
[d] IRIS S.r.l., Via Giovanni Paolo II, 26, 10043 Orbassano (TO), Italy

ARTICLE INFO

Keywords:
Bioactive glasses
Plasma treatment
Antiadhesive properties
Bioactivity

ABSTRACT

The development of antimicrobial and anti-adhesive surfaces presents a significant challenge in the advancement of biomaterials, particularly in the context of bioactive materials for bone substitution. This research focuses on the deposition of an anti-adhesive coating using an atmospheric dielectric barrier discharge plasma technology for the surface of two bioactive glasses, SBA2 and S53P4. The obtained materials were characterized from a morphological-compositional point of view, evidencing a uniform coating with a pillar structure. The surface properties, investigated through wettability, roughness, and zeta potential analyses, showed an increased hydrophobicity and the exposition of $-NH_2$ groups. Moreover, since the presence of the coating and plasma treatment can interfere with the bioactivity mechanism, in vitro bioactivity test was performed, highlighting an increased bioactivity kinetics. The surface adhesion behavior of a Multidrug-resistant bacterial strain, *Staphylococcus aureus,* was estimated by exploiting a preliminary test after 90 min of incubation. The results showed a significant decrease in the colonies attached to the surfaces for both treated glasses compared to the pristine samples. This decrement in bacterial attachment is attributed to the conferment of hydrophobic properties, with a possible role also played by the obtained roughness. This study presents an innovative approach that integrates atmospheric plasma surface modification with bioactive glass technology to develop bone substitute materials that both prevent bacterial colonization and maintain their regenerative capabilities.

1. Introduction

The development of advanced materials for biomedical applications has gained significant attention in recent years, particularly in the field of bioactive glasses. These materials are known for their bioactivity and ability to chemically bond with bone, making them suitable for various implantable devices. However, a critical challenge in the application of bioactive glasses is their susceptibility to biofouling, a multi-stage process that involves the initial adsorption of organic molecules and subsequent microbial colonization, until the formation of a biofilm. Particularly, the mechanism of bacterial adhesion begins with a reversible adsorption phase driven by weak physical forces, such as electrostatic forces, van der Waals interactions, and hydrophobic effects. These events encourage the transitory attachment of planktonic bacteria to surfaces, not compromising their ability to detach. Afterwards, it is shown a stronger primary adhesion through bacterial surface structures, e.g. fimbriae, adhesins, or lipopolysaccharides, resulting in the irreversible attachment and biofilm formation [1–3]. This process can lead to complications such as bone infection and implant failure [4,5]. To address this issue, the surface modification of such materials to impart anti-adhesive or antimicrobial properties is essential.

Several techniques have been investigated to achieve antibacterial or anti-biofouling properties on bioactive glass surfaces [6–16]. incorporating chemical agents onto the material's surface via various interactions and altering the surface properties (morphology, charge…) represent the most investigated procedures [6].

As example, the enrichment of bioactive glass surfaces with antimicrobial ions, such as Ag^+, Zn^{2+}, and Cu^+ [7,8], or nanoparticles [9,10].

* Corresponding author.
E-mail address: marta.miola@polito.it (M. Miola).

https://doi.org/10.1016/j.surfin.2026.108515
Received 4 February 2025; Received in revised form 18 December 2025; Accepted 15 January 2026
Available online 16 January 2026

has been widely explored to reduce bacterial adhesion. Antimicrobial activity has been imparted using different methods, from the ion-exchange technique [7,8]. to in situ reduction of nanoparticles [10, 11], or sonochemical procedure in combination with thermal treatment [12]. Antimicrobial properties can also be achieved by incorporating antibacterial drugs or biomolecules on bioactive glass surfaces, including lysozyme and antibiotics [13,14].

Concerning the realization of anti-adhesive materials through surface properties modification, in the literature, there are few works regarding bioactive glasses; however, for example, Shaikh et al. utilized a femtosecond laser to modify the surface roughness, wettability, and chemical composition, thereby reducing bacterial attachment and biofilm formation on 45S5 Bioglass® [15]. Another work reported the development of mesoporous bioactive glass with anti-adhesive zwitterionic surfaces by a co-grafting of $–NH^{3\pm}COO^{-}$ surface groups [16]. Recently, the authors proposed a plasma deposition of hexamethyldisiloxane to impart anti-adhesive properties [17].

Whereas, this work concerns the use of the atmospheric dielectric barrier discharge plasma technology to modify a coating applied to bioactive glasses, consisting of an antiadhesive fluoroalkyl-functional water-borne oligosiloxane. This oligosiloxane is recognized for its low surface energy, which imparts hydrophobic properties and reduces the adhesion of microorganisms [18–21]. In particular, in this work, the non-thermal plasma technology has been investigated to improve the adhesion of the coating, allow its polymerization and tailor the chemical and morphological properties of the surface, conferring an antiadhesive effect. Two bioactive glass compositions have been selected and compared: a commercial one (S53P4, commercially known as BonAlive®) and a second composition previously designed by the authors. Plasma technology to impart or enhance antibacterial/antiadhesive properties to biomaterials has been addressed in the literature; however, to the best of our knowledge, the use of thermal atmospheric plasma technology on bioactive glasses is still little explored. However, this technique has several advantages because it allows modulation of surface properties from the macro to the atomic scale.

This paper explores the relationship between plasma processing parameters and the resulting surface properties, including hydrophobicity, topography, biocompatibility, and bacterial adhesion [18–21]. The application of plasma technology, still little investigated in the field of bioactive ceramics, allows enhancing the uniformity and stability of the coating, thereby improving its performance in a biological environment. The findings of this research are expected to contribute to the development of more effective biomaterials that can mitigate the risks associated with biofouling while maintaining the desirable properties of bioactive glasses.

2. Materials and methods

2.1. Materials

For the synthesis and plasma modification of bioactive glasses the following reagents were used: silica (SiO_2 – Sigma Aldrich, Cat. No: 83,340, purum p.a., Germany), sodium carbonate (Na_2CO_3 – Sigma Aldrich, Cat. No: 222,321, ACS reagent, anhydrous, ≥99.5 %, Germany), calcium carbonate ($CaCO_3$ - Sigma Aldrich, Cat. No: 239,216, ACS reagent, ≥99.0 %, Germany), calcium phosphate ($Ca_3(PO_4)_2$ – Sigma Aldrich, Cat. No: 21,218, purum p.a., ≥96.0 %, Germany), alumina (Al_2O_3 – Thermo Fisher Scientific, Cat. No: 042,573.36, ≥99.95 %, USA), boric acid (H_3BO_3 – Sigma Aldrich, Cat. No: B0394, ACS reagent, ≥99.5 %, Germany) and DYNASYLAN ® F 8815 (Evonik Operations GmbH, Germany).

2.2. Sample preparation

In this study, two bioactive glasses compositions, belonging to 53 % SiO_2, 23 % Na_2O, 20 % CaO, 4 % P_2O_5, wt % (S53P4, commercially known as BonAlive®) and 48 % SiO_2, 18 % Na_2O, 30 % CaO, 3 % P_2O_5, 0.43 % B_2O_3, 0.57 % Al_2O_3, mol % (SBA2), were synthesized by melting the reactants in a Pt crucible at 1450 °C for 1 h (SBA2) and 1360 °C for 3 h (S53P4) and quenching the melt in a cylindrical brass mould. SBA2 was annealed at 500 °C for 13 h and S53P4 at 520 °C for 1 h, according to other protocols [22,23]. Afterward, the obtained bars were cut into slices of 10 mm in diameter and 4 mm in height, which were polished with SiC abrasive papers ranging from 800 to 4000 grits to uniform the surfaces. The two bioactive glass compositions were selected with the purpose of comparing a composition developed by the authors and a commercial one.

2.3. Surface modification

The obtained glasses were then coated with a commercial fluoroalkyl functional water-borne oligosiloxane (DYNASYLAN ® F 8815, Evonik Operations GmbH, Germany) and atmospheric plasma-treated to obtain an anti-adhesive surface. The samples were immersed in a solution of F8815 and methanol (10 % v/v) and left to dry for 24 h. Afterward, all glasses were subjected to an Ar plasma treatment, using a reactor in dielectric barrier discharge (DBD) at room temperature for 45 s, using a frequency of 5 kHz and a voltage of 6 kV, to increase the adhesion of the coating, allow its polymerization and modify the surface in terms of morphology and functional groups, useful for inhibiting bacterial adhesion. From now on, the untreated samples will be called SBA2_NT and S53P4_NT, while the treated ones SBA2_T and S53P4_T.

2.4. Sample characterization

2.4.1. Morphological and compositional characterization

The surface of the glasses, both before and after treatment, was investigated from a morphological and compositional point of view by field emission scanning electron microscopy (FESEM SUPRA TM40, Zeiss, Germany) equipped with energy dispersive X-ray spectroscopy (EDS). Glasses were coated with a thin Pt layer before FESEM observation.

Moreover, the presence of the F8815 and the functional groups exposed on the glass surface was investigated through the Attenuated Total Reflection Fourier Transform IR (ATR-FTIR) spectroscopy (Nicolet iS50 FTIR Spectrometer, Thermo Fisher Scientific, United States of America). The spectra were acquired in the range 400–4000 cm^{-1} with a resolution of 4 cm^{-1} with 32 scans for each spectrum. OPUS software (v. 6.5, Bruker S.p.A) was adopted for instrumental control and spectral acquisition.

2.4.2. Surface properties characterization

To investigate the topographical features of the glasses, a laser optical profilometer (LSM 900, Zeiss, Germany) was used to determine the surface pattern and roughness parameters, specifically Sa, with a 20x objective, using the Confomap software. The measurements were performed on uncoated glasses, dip-coated glasses and glasses after plasma treatment to better examine the effect of plasma on the coating.

The modification of the surface wettability was analysed with a static contact angle (DSA 100, Krüss, Germany), using the sessile drop technique and water (WCA). For each glass, three measurements were evaluated on two different samples; the value of the contact angle was automatically measured after 2 s. Results are reported as average ± standard deviation (SD).

The surface charge in function of pH of pristine samples and after the dip coating process and plasma treatment was investigated by measuring the zeta potential, using an electrokinetic analyser (SurPASS, Anton Paar, Austria) equipped with an adjustable gap cell, an automatic titration unit, and KCl 0.001 M was used as electrolyte. pH was adjusted by automatic addition of HCl 0.05 M and NaOH 0.05 M for the acid and basic range, respectively. Separate sets of samples were utilized for acidic and basic titrations to prevent any reactions from affecting the

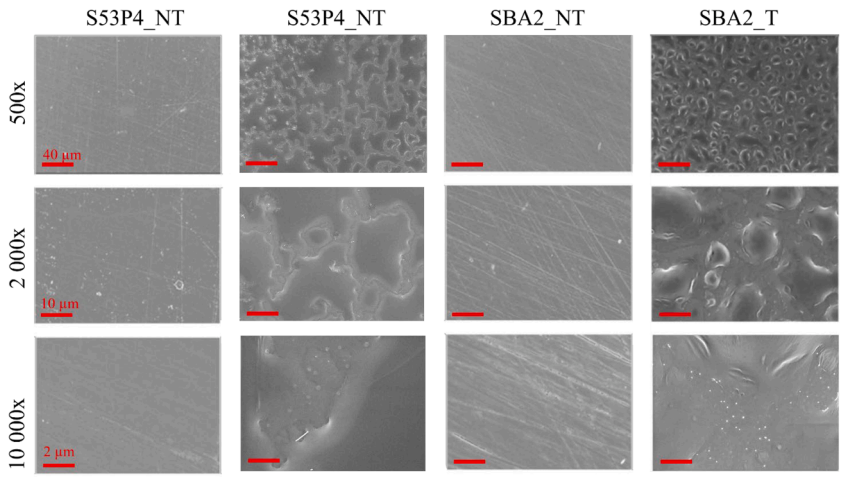

Fig. 1. FESEM micrographs of SBA2_NT, SBA2_T, S53P4_NT and S53P4_T at 500x, 2kx and 10kx.

measurements.

2.4.3. In vitro bioactivity test

Since the presence of a coating and the subsequent plasma treatment can interfere with the mechanisms of the bioactivity process, in vitro test, before and after the treatment for SBA2 and S53P5 glasses, were carried out by dipping samples in 50 ml of simulated body fluid (SBF – Kokubo protocol [24]) maintained at 37 °C and 120 rpm for 3, 7, and 14 days.

At the end of each incubation time, the pH of the solution was measured, the glasses were removed from the SBF solution, rinsed in bi-distilled water, and dried at room temperature. Subsequently, the precipitation of hydroxyapatite (HA) was analysed employing FESEM-EDS and X-Ray diffraction (XRD - X'Pert diffractometer, Philips). FESEM-EDS analyses were carried out as previously described; XRD investigation was performed using the Bragg-Brentano camera geometry with Cu Kα incident radiation, with a 2θ range from 10° to 70° The obtained spectra were analysed with software (X'Pert High Score, Philips, Netherlands) equipped with PCPDFWIN database.

2.4.4. Anti-adhesive evaluation of samples on staphylococcus aureus

The evaluation of surface modifications for bacterial adhesion was performed against Multidrug-resistant *Staphylococcus aureus* (MDR *S. aureus*), a main concern for bone implant infections. Due to its resistance to several antibiotics, including methicillin and oxacillin, and its ability to form biofilms on implant surfaces, combating this bacterium poses a considerable challenge for physicians and surgeons [25]. MDR *S. aureus* was purchased from the American Type Culture Collection (ATCC, ATCC 43,300). Following the manufacturer's instructions, it was cultivated in Luria Bertani (LB) agar/broth medium and incubated at 37 °C for 24 h to promote bacterial growth. The growth was quantified by measuring the optical density (OD) of LB broth at a wavelength of 600 nm using a spectrophotometer, where $OD_{600nm} = 0.001$ corresponded to 1×10^5 CFU/mL (colony-forming unit/mL) [26].

The anti-adhesive effect of the sample's surface treatments against MDR *S. aureus* was evaluated by exposing bacterial cells to the treated surfaces, following the protocol of the International Organization for Standardization (ISO 22,196:2011, titled 'Measurement of antibacterial activity on plastics and other non-porous surfaces'). Briefly, 50 µL of a bacterial suspension containing 1×10^5 CFU/mL was applied to the sterilized sample surfaces. The samples had been sterilized using UV-C light for 30 min on each side. The samples were then incubated at 37 °C for 90 min to allow bacterial attachment to the surfaces.

According to the literature, the transition from reversible to irreversible bacterial attachment on surfaces typically occurs within 90–120 min [27]. Subsequently, the samples were washed once with phosphate-buffered saline (PBS) to remove non-adherent bacteria. The number of viable surface-adhered bacterial colonies and their morphology were assessed using CFU count and FESEM.

For CFU counting, bacterial cells were detached from the sample surfaces by adding 0.5 % Tween solution and incubating for 30 min. This was followed by three cycles of sonication (5 min each) and vortexing (20 s each). Six ten-fold serial dilutions were prepared by transferring 20 µL of the detached bacterial suspension into 180 µL of PBS. Finally, 20 µL from each serial dilution was plated on LB agar and incubated at 37 °C for 24 h. Colony counts were used to calculate the CFU number using the following formula [28].

$$CFU = [colony\ number \times dilution\ factor]^{serial\ dilution}$$

The morphology of surface-adhered bacterial cells and microbiofilms was further analysed using FESEM, as described in section 2.3.1. SMILEVIEWTM Map software (version 8.2.9621, JEOL) was used to modify the captured FESEM images and distinguish bacterial cells clearly from the sample surface.

2.4.5. Statistical analysis

Statistical analysis of the obtained results was conducted using the SPSS software (v.20.0, IBM). Normal distribution and homogeneity of variance were confirmed using Shapiro-Wilk's and Levene's tests, respectively. Differences between groups were analysed using the paired Student's *t*-test. Significant differences were set at p-values <0.05 and <0.01, indicated here by * and **, respectively.

3. Results and discussion

3.1. Morphological and compositional characterization

Fig. 1 reports the morphology of the pristine glasses (NT) and after the coating with polymer and plasma treatment (T). As it can be noticed, the surface of the glasses SBA2_T and S53P4_T appears rougher, and the presence of a coating is observed, although with a different morphology. On SBA2_T glass, a drop-like morphology is observed, while on S53P4_T glass, the raised areas seem more connected. The compositional analysis (Fig. 2) highlights the characteristic peaks of the glasses, in particular Si, Ca, Na, and P, and in addition, the F peak (indicated by arrows) for the samples subjected to dip-coating and plasma treatment. Fig. 2 shows a spectrum and an image of the analyzed air as an example, along with the table displaying the average atomic and weight percentages.

The FTIR analysis of pure polymer is reported in Fig. 3a; the spectrum evidences the characteristic peak of F8815: at about 3335 cm^{-1} a large band ascribable to Si-OH group, at 1639 cm^{-1} an intense peak due to NH_2 stretching, two peaks at about 1241 and 1206 cm^{-1} attributed to

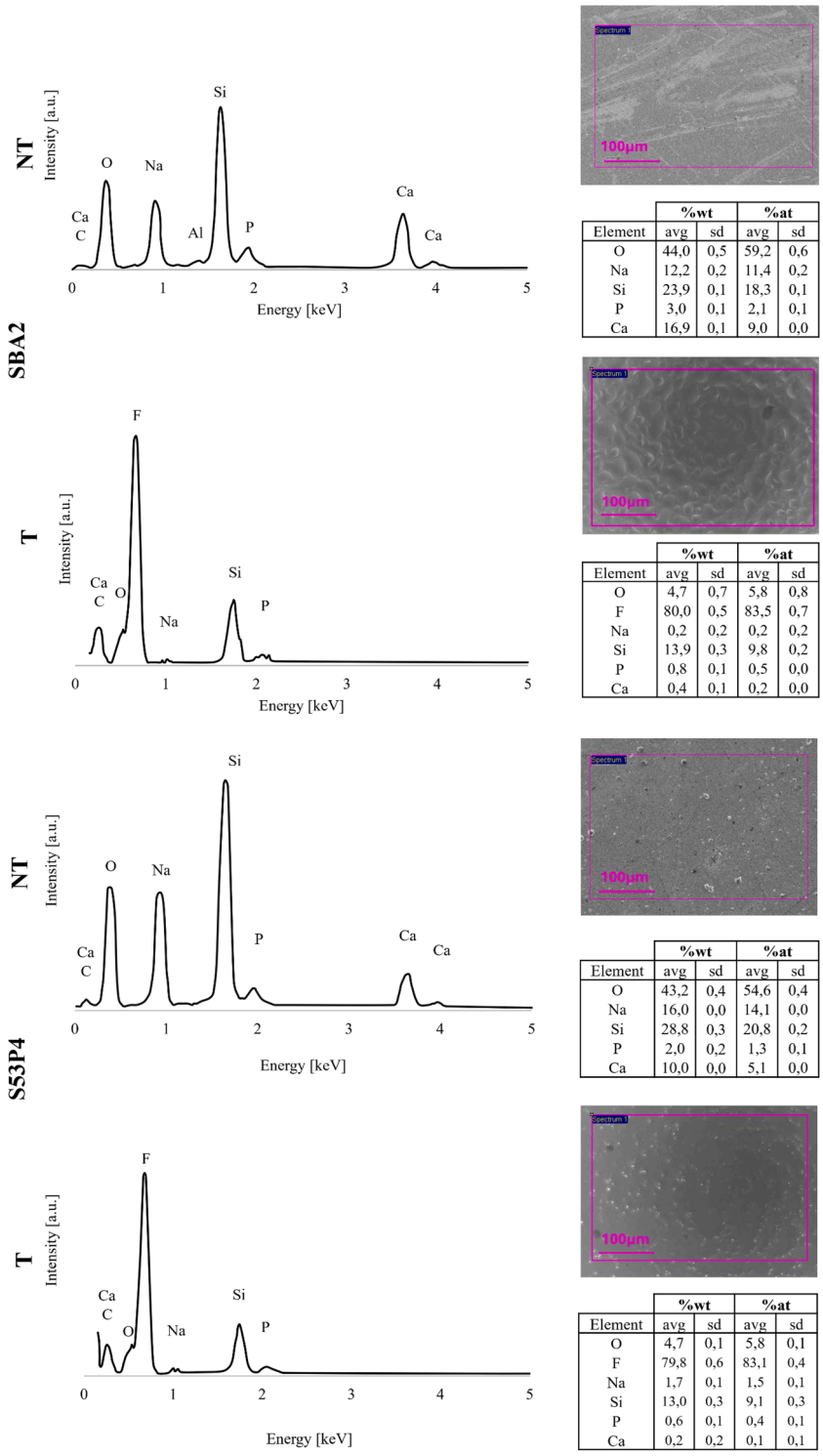

Element	%wt avg	%wt sd	%at avg	%at sd
O	44,0	0,5	59,2	0,6
Na	12,2	0,2	11,4	0,2
Si	23,9	0,1	18,3	0,1
P	3,0	0,1	2,1	0,1
Ca	16,9	0,1	9,0	0,0

Element	%wt avg	%wt sd	%at avg	%at sd
O	4,7	0,7	5,8	0,8
F	80,0	0,5	83,5	0,7
Na	0,2	0,2	0,2	0,2
Si	13,9	0,3	9,8	0,2
P	0,8	0,1	0,5	0,0
Ca	0,4	0,1	0,2	0,0

Element	%wt avg	%wt sd	%at avg	%at sd
O	43,2	0,4	54,6	0,4
Na	16,0	0,0	14,1	0,0
Si	28,8	0,3	20,8	0,2
P	2,0	0,2	1,3	0,1
Ca	10,0	0,0	5,1	0,0

Element	%wt avg	%wt sd	%at avg	%at sd
O	4,7	0,1	5,8	0,1
F	79,8	0,6	83,1	0,4
Na	1,7	0,1	1,5	0,1
Si	13,0	0,3	9,1	0,3
P	0,6	0,1	0,4	0,1
Ca	0,2	0,2	0,1	0,1

Fig. 2. EDS analysis of SBA2_NT, SBA2_T, S53P4_NT, and S53P4_T: EDS spectrum, table showing at % and wt % of the elements and image of the analyzed area.

the C-F stretching, and a peak at about 1070 due to Si-O bond [29]. The spectra of untreated and treated samples (Fig. 3b) show the typical peak of silica-based bioactive glasses: at about 750 cm^{-1} and 1000–1200 cm^{-1} the bands ascribable respectively to the Si-O symmetric stretching and the asymmetric stretching of Si-O-Si bonds, and a band at 850 - 950 cm^{-1} related to SiO_4 tetrahedron structures containing non-bridging oxygen. Following glass coating and plasma treatment, the band relating to the Si-OH bond disappears; this highlights that the bond with the glass occurs through the silanol groups. However, if we take into consideration the spectrum in the region of the OH groups (inset in Fig. 3b), we can notice a difference between the dip-coated samples and the plasma-treated ones. On samples subjected only to the dip coating process, the presence of -OH groups is still observed, while on plasma-treated samples, this band disappears, suggesting a uniform polymer coating after plasma treatment, a complete bonding of the polymer with the substrate and its polymerization. However, further specific surface characterizations are needed to confirm the results obtained by FTIR analysis. Moreover, the treated glasses display the band

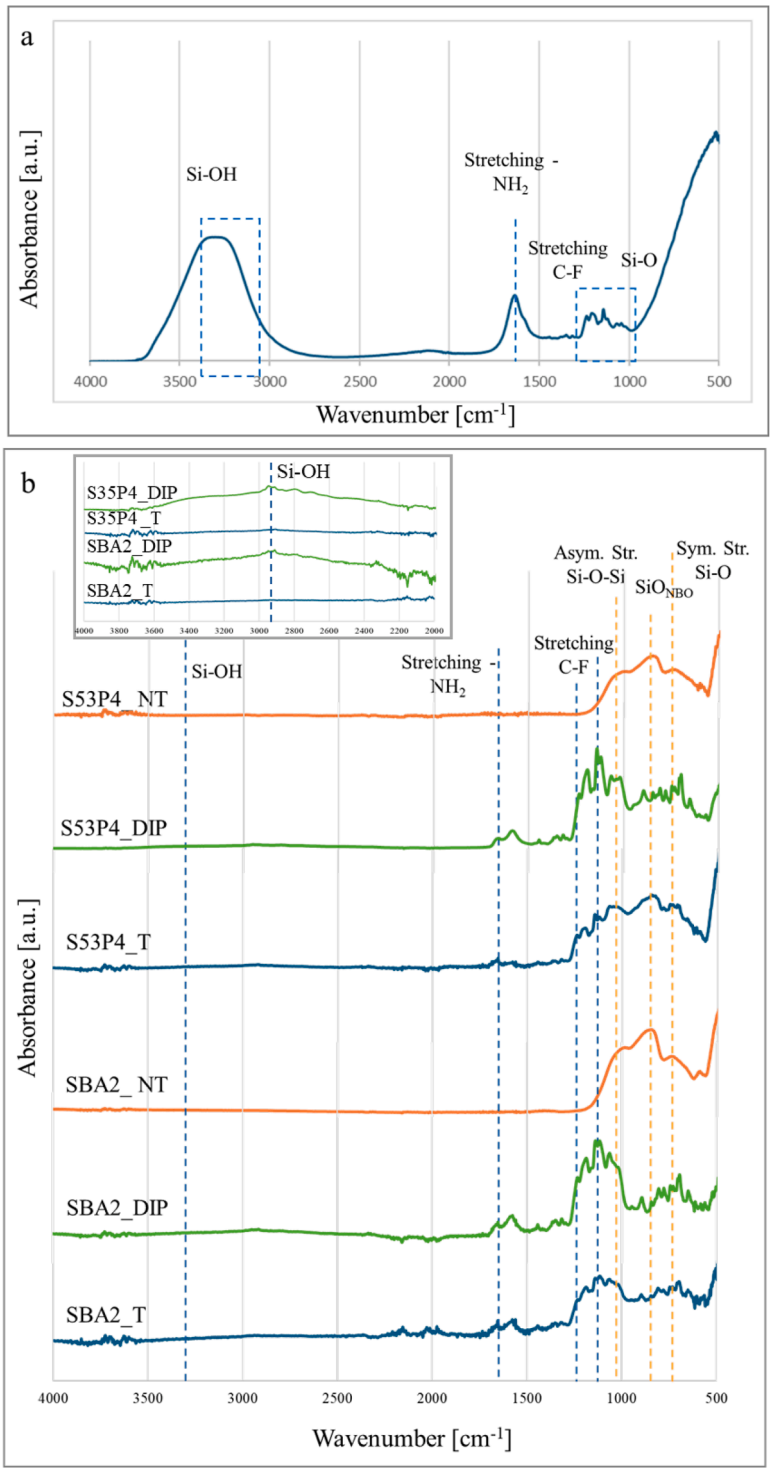

Fig. 3. FTIR spectra of a) pure F8815 monomer, b) pristine SBA2 and S53P4 glasses (NT), after dip coating (DIP), and after dip-coating and plasma treatment (T).

at 1639 cm^{-1} due to the stretching of the NH_2 group; the other peaks, particularly those ascribable to the C-F stretching and the Si-O bond between 1250–1000 cm^{-1}, are partially overlapped with the characteristic bands of the glasses. Anyway, the surface modification of the glass due to the coating and plasma treatment is visible on both samples.

3.2. Surface properties characterization

In Fig. 4, the mean and standard deviation of the static contact angle measurements are reported. The contact angles of the SBA2_T and S53P4_T samples are significantly higher than the pristine glasses (t-test, $p < 0.05$ for SBA2, $p < 0.0001$ for S53P4), particularly that of the S53P4_T. The achieved values are not exactly typical of hydrophobic surfaces (static water contact > 90°), but it must be underlined that a high hydrophobicity may not also allow protein adsorption and cell adhesion [30]. Too high hydrophobicity can affect the type and conformation of the ECM adsorbed proteins and, consequently, cell adhesion. Cell attachment also depends on the cell type; for example, as reported by some authors, a contact angle between 60° and 90° improves fibroblast adhesion, while the adhesion of osteoblasts decreases

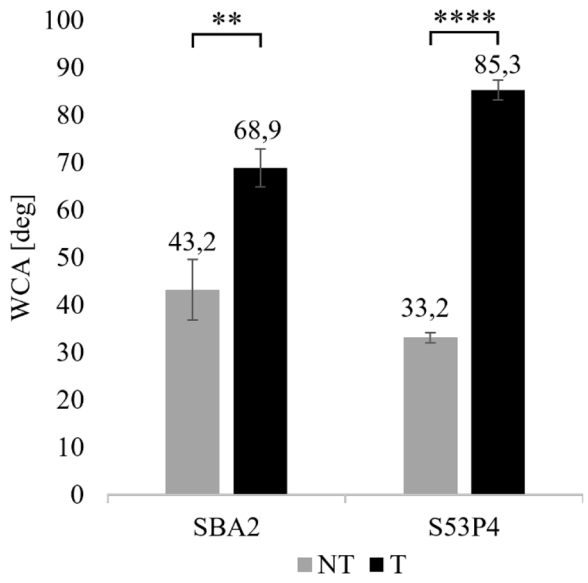

Fig. 4. Contact angle measurements of pristine SBA2 and S53P4 glasses (NT) and after dip-coating and atmospheric plasma treatment (T).

from 0° to 106° Therefore, the obtained values can be a good compromise, useful for limiting bacterial adhesion without impairing cellular adhesion [30,31].

Three-dimensional images of the glasses' surface were obtained using confocal microscopy and are displayed in Fig. 5. As can be observed, the deposition of the coating confers a certain roughness to the surface with the formation of non-uniform pillars. The subsequent plasma treatment generates a more homogeneous pattern on the surface of the samples characterized by micropillars. Therefore, plasma treatment has a significant effect on the morphology of the coating, creating a uniform surface with the presence of pillars. The latter, together with hydrophobicity, can have a role in inhibiting bacterial adhesion.

Moreover, since the roughness of the materials is a parameter of fundamental importance that regulates bacterial and cellular adhesion, the roughness values (Sa) of the glasses before and after treatment were also evaluated (Table 1). In particular, some works have highlighted that roughness on both the nanometric and microscale can influence bacterial adhesion [32]. As can be seen, the roughness slightly increases after the dip coating process and subsequently also after the plasma treatment, while remaining on a nanometric scale.

The roughness values that inhibit bacterial adhesion are still debated in the literature, also because they are closely related to the topography and the investigated strain [32,33]. However, some studies have shown that extremely low Sa (< 10 nm) values or between 45 and 390 nm limit bacterial adhesion, while micro-scaled materials or Sa values between 10 and 40 nm increase it [32,33]. Therefore, the obtained roughness and topography can play a role in the antibacterial and antifouling properties of the plasma-treated bioactive glasses (in addition to the low observed wettability), since, as observed by other authors [34,35], a patterned surface can inhibit the bacteria's adhesion and the subsequent formation of biofilm.

Zeta potential titration curves of pristine and treated bioactive glasses are reported in Fig. 6.

The isoelectric point of SBA2_NT is 3.1, and that one of S53P4 is lower than 3, as previously reported by the authors [36] and in accordance with literature [37]. The acidic value of the isoelectric point is due to the presence of surface acidic groups as -OH groups for bioactive glasses. The presence of acidic groups, fully deprotonated from pH 6 on, is confirmed by the presence of a plateau in the basic region. Due to the acidic isoelectric point, bioactive glasses show a negative surface charge in almost all the explored pH range.

After the treatment, a significant change can be observed for both materials. The curves are similar and positive throughout the whole explored pH range. This result suggests the presence of a homogeneous layer, analogous to both bioactive glasses, characterized by basic groups. The presence of basic functionalities, fully protonated below pH

Table 1
Roughness (Sa) values of SBA2 and S53P4 not treated, dip-coated, and treated with plasma obtained by ISO 25178.

	NT	Dip-coated	Dip-coated + Plasma
SBA2	82 nm	160 nm	180 nm
S53P4	89 nm	161 nm	286 nm

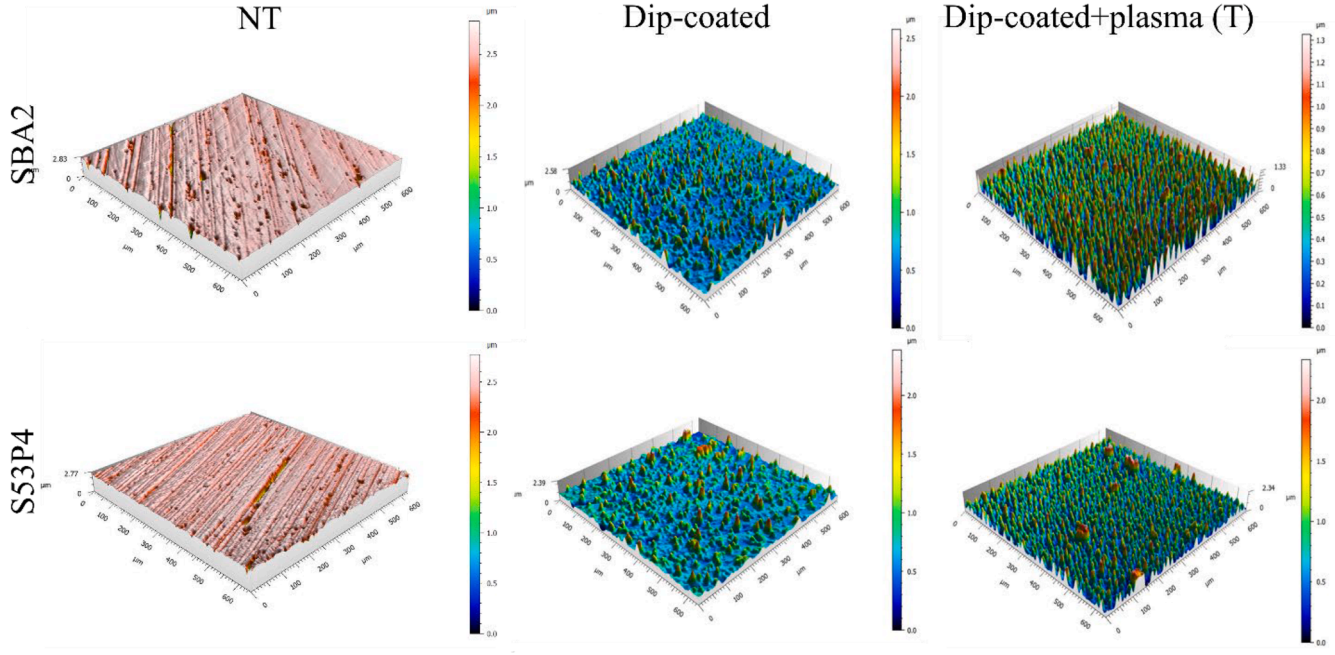

Fig. 5. Optical profilometry 3D images of the surface of the pristine (NT), dip-coated, and plasma-treated SBA2 and S53P4.

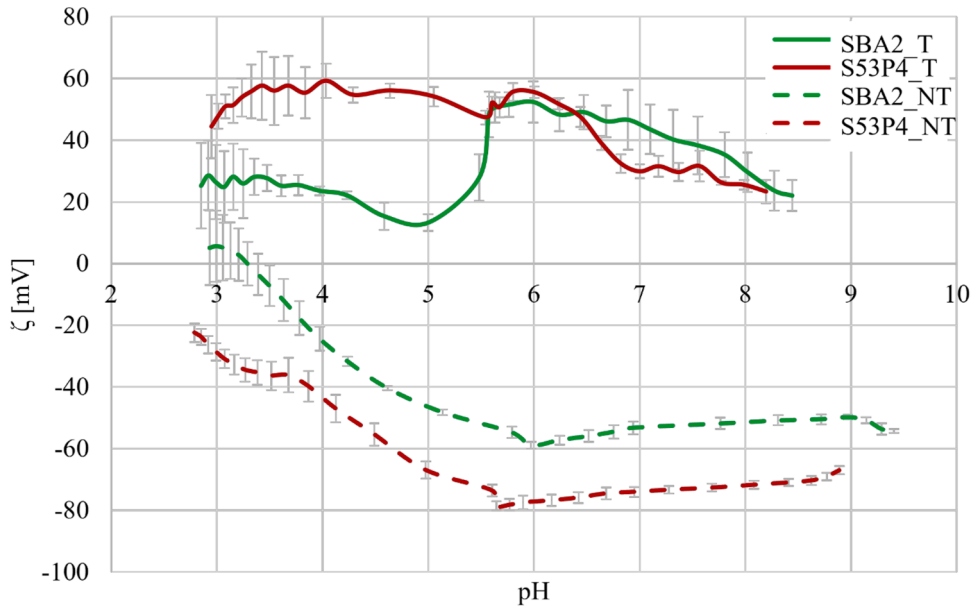

Fig. 6. Zeta potential titration curves of pristine and treated bioactive glasses.

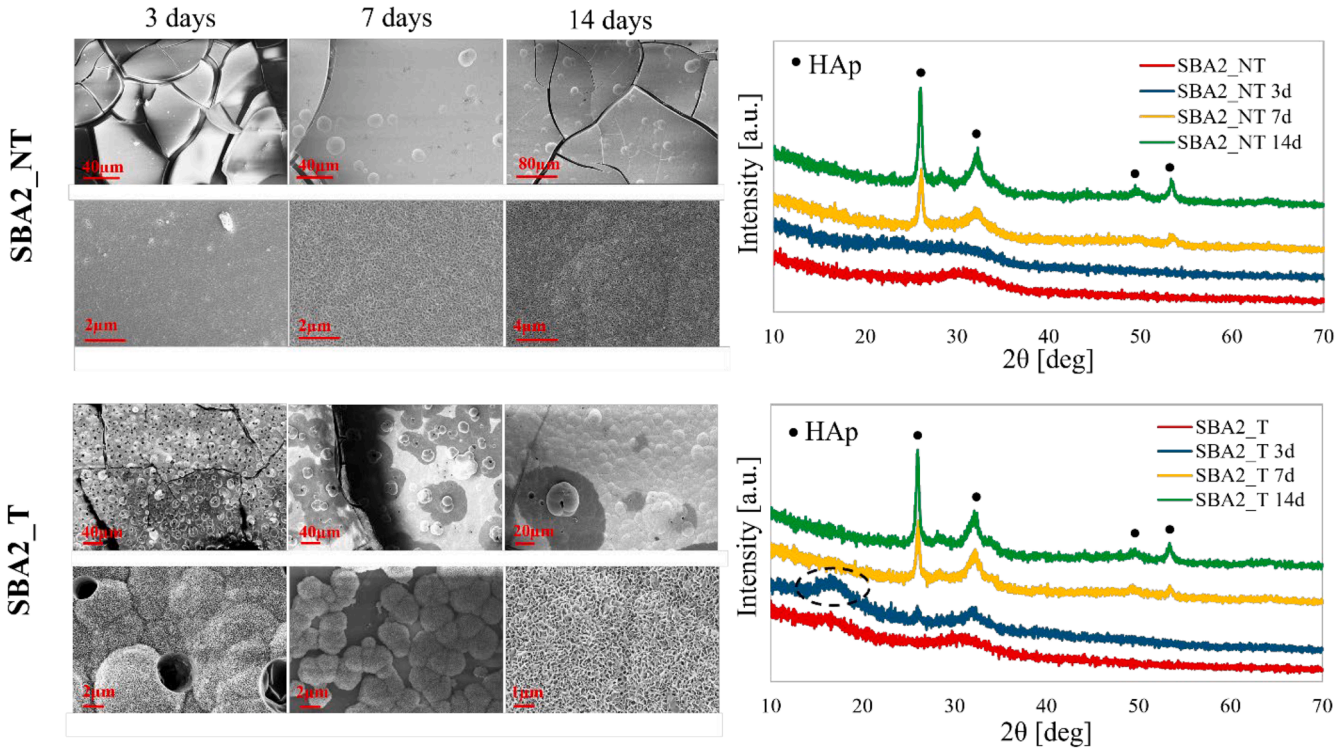

Fig. 7. FESEM micrographs and XRD spectra of SBA2_NT and SBA2_T after 3, 7, and 14 days of SBF immersion.

6, is confirmed by the plateau in the acidic region.

The prevalence of basic groups (-NH_2) after treatment is in accordance with the above-discussed FTIR results. However, as previously mentioned, other surface-sensitive characterizations could be useful to confirm this hypothesis and confirm the exposure of the amino groups only.

3.3. *In vitro bioactivity test*

The bioactivity of the treated glasses, in comparison with the untreated ones, is reported in Figs. 7 and 8. Fig. 7 shows the FESEM images and XRD spectra of SBA2_NT and SBA2_T. After 3 days of immersion in SBF, the presence of silica gel and of the first hydroxyapatite nuclei is noticed, particularly on the treated sample. Cracks are visible across the silica gel layer due to the extraction of the glasses from the solution, the drying process, and the vacuum that is required for FESEM observations. The apatite layer grows over the next few days on both samples. On SBA2_T glass, the apatite layer seems to grow between the polymer pillars; in fact, darker areas rich in fluorine were observed (EDS analysis not reported). XRD analyses confirm a faster bioactivity kinetics for the SBA2_T sample. Indeed, the peaks relating to hydroxyapatite (HAp) are visible already after 3 days of immersion, together with the silica gel

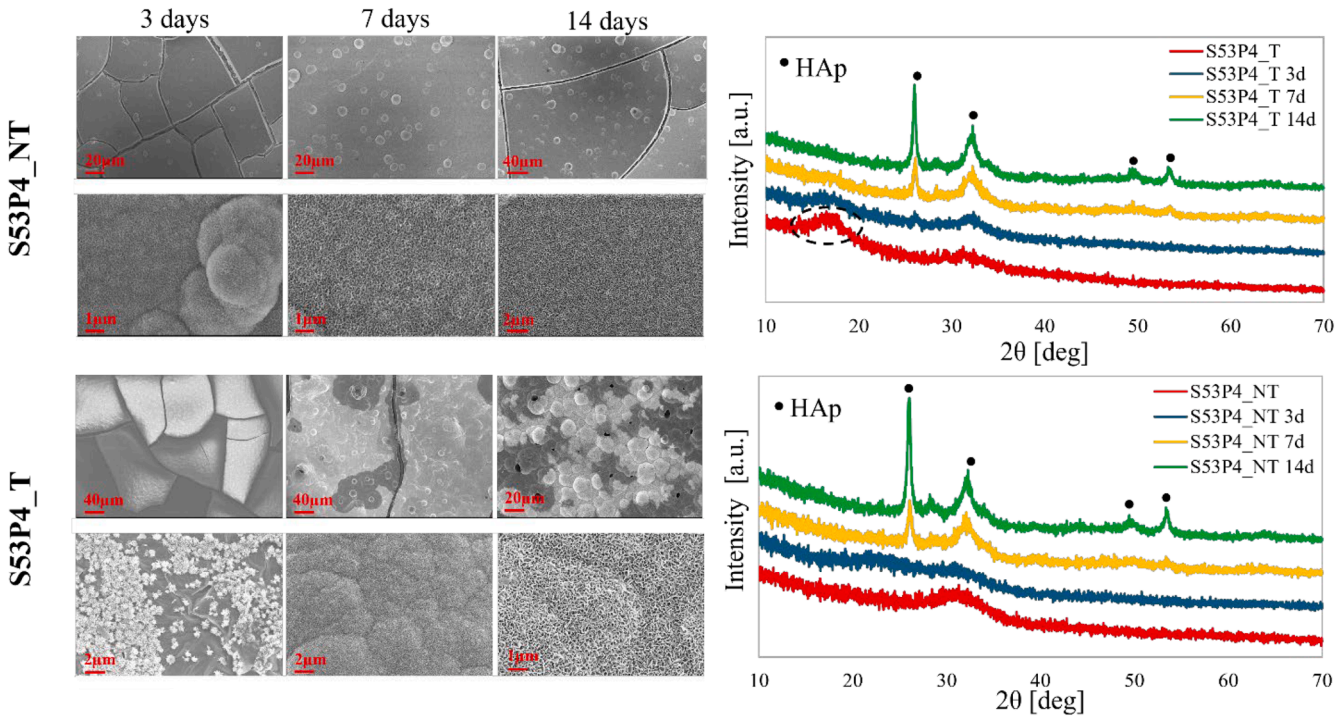

Fig. 8. FESEM micrographs and XRD spectra of S53P4_NT and S53P4_T, and after 3, 7, and 14 days of SBF immersion.

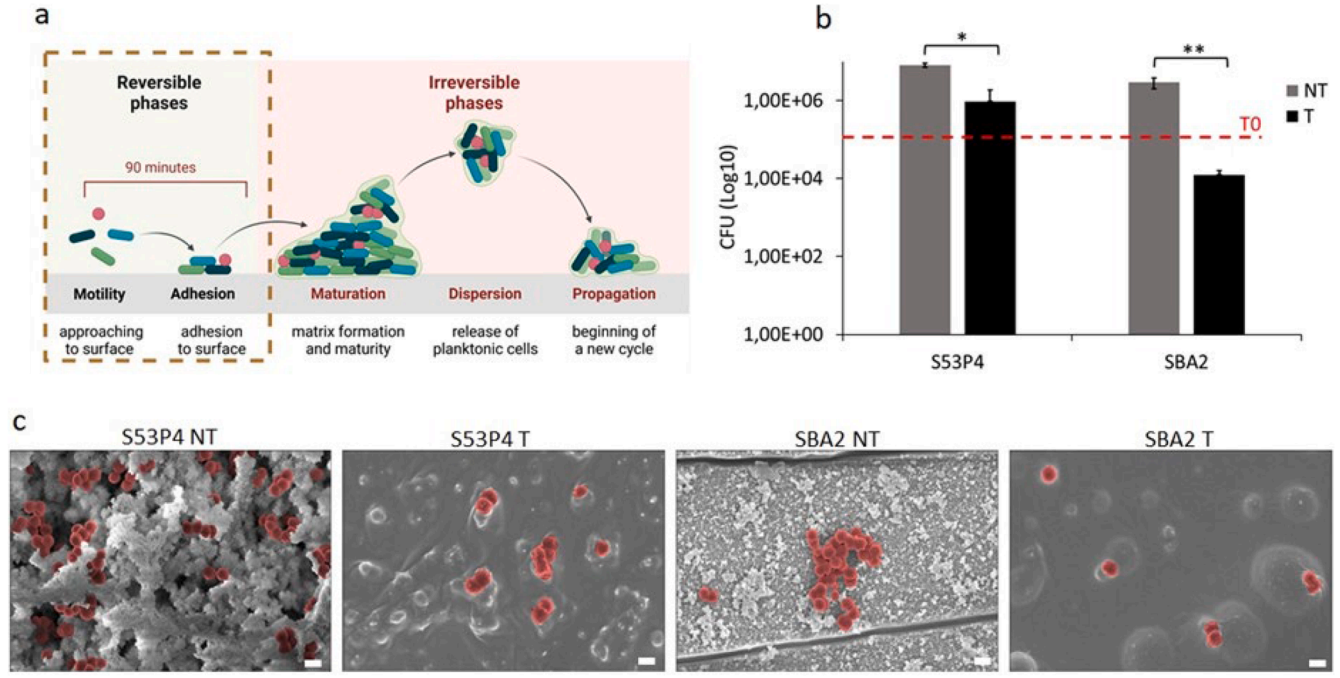

Fig. 9. Anti-adhesive evaluation of the samples against MDR *S. aureus* after 90 min of incubation. a) Schematic description of biofilm formation; b) The viable surface-adhered bacterial number (CFU count), the red line shows the initial number of bacteria (1×10^5 CFU/mL); * and ** indicate p-value<0.05 and <0.01, respectively; c) FESEM images; bacterial cells were colored in red suing SMILEVIEW™ map software, scale bar = 1 μm.

halo, highlighted with a dotted circle in the figure.

Even for S53P4 glass (Fig. 8), a faster bioactivity kinetics for the treated glass can be observed both from the images obtained at FESEM and from the X-ray spectra. Indeed, after 3 days of SBF immersion, the surface of S53P4_T samples is covered by a silica gel layer (evidenced by a dotted circle in XRD spectrum) that incorporates HAp; while on S53P4_NT sample surface, the presence of apatite nuclei is not observed for the same time frame, but only after 7 days. Therefore, for both glasses, the presence of the coating seems to increase the speed of HAp nucleation. This can be due to the presence of the NH_2 group on the surface of glasses. As reported by other authors [38], the presence of different functional groups (both with negative and positive charge) on the surface of biomaterials can influence the deposition of hydroxyapatite. In particular, the NH_2 group can favour the deposition of HAp due

to an electrostatic attraction of PO_4^{3-} ions.

3.3. Antibacterial test

3.3.1. Anti-adhesive evaluation of samples against staphylococcus aureus

Due to the multidrug-resistant and biofilm-forming ability of MDR *S. aureus* on bone implants, dealing with this bacterial strain has always been a major concern following surgical operations. Bacterial adherence on surfaces, facilitated by reversible chemical bonds such as hydrogen, ionic, and covalent bonds, is the first step in biofilm formation. Subsequently, bacteria use surface proteins such as accumulation-associated proteins, autolysins, wall teichoic, and lipoteichoic acids to adhere irreversibly and create micro-colonies on medical devices [39]. Afterward, the biofilm layer matures and disperses, meaning the micro-colonies grow and some single bacterial cells are released from the mature biofilm (Fig. 9a)[40]. In line with previous literature, 90 min was selected as the time required for firm or irreversible bacterial attachment to the surfaces. For example, Sharifikolouei et al. (2021) evaluated the antifouling properties of superhydrophobic zirconium-copper-based metallic glass thin films (Zr-Cu-Ag) against *Staphylococcus aureus* (Gram-positive) and *Escherichia coli* (Gram--negative). Bacterial adhesion and metabolic activity were assessed after 90 min (early time point) and 24 h (late time point) of exposure to the samples' surfaces. The results demonstrated a significant reduction (about 95 %) in both parameters after 90 min compared to 24 h [41].

To evaluate the effect of modifications of bioactive glasses (SBA2 and S53P4) using polymer and plasma treatments on surface-adhered bacteria, MDR *S. aureus* was applied to the sample surfaces and incubated at 37 °C for 90 min. After incubation, the number of surface-adhered bacterial colonies was calculated using colony-forming unit (CFU) counting, and the results are presented in Fig. 9b–c. As explained in section 2.3.4, the initial number of bacteria used for the experiment was 1×10^5 CFU/mL, indicated by the red line in Fig. 9b CFU counts showed a statistically significant decrease in the number of viable surface-adherent bacterial colonies on the treated samples: approximately a 1-Log reduction for S53P4 T and >2-Log reduction for SBA2 T compared to the pristine samples, S53P4 NT, and SBA2 NT (control). After 90 min of incubation, the number of bacterial colonies attached to the surfaces of SBA2 T was noticeably lower than the initial number of bacterial colonies (Fig. 9b; * and ** represent p-value$<$0.05 and p-value$<$0.01, respectively). These findings were confirmed by visualizing the samples' surfaces using FESEM, which demonstrated only a few single bacterial cells on the surfaces of the S53P4 T and SBA2 T samples. In contrast, the pristine samples exhibited a significantly higher number of bacterial cells, such as S53P4 NT, or aggregates of bacterial cells as seen on SBA2 NT (Fig. 9c; bacterial cells were coloured red using SMILEVIEW™ map software, JEOL, Japan). As described above, the surface characteristics after coating and plasma treatment of the pristine samples showed a drastic effect on the wettability, roughness, and topography of the samples' surfaces, which, in combination with each other, can decrease the bacterial adherence to the surfaces. In line with previous literature, increasing the contact angles from hydrophilic to hydrophobic (from 33.2 to 85.3 for S53P4 T) can hinder bacterial attachment by reducing the available surface area for bacterial adherence [42]. Additionally, as reported in the literature, modifying the nanometric roughness of the surface to below 200 nm (Ra SBA2 = 180 nm) can significantly reduce bacterial adherence due to the smoother surface and lack of strong contact points [43]. The anti-adhesive effect can be mainly attributed to the reduced wettability; additionally, the topographical features generated through plasma treatment may have further contributed to inhibiting bacterial adhesion. However, more in-depth analyses are necessary to compare and distinguish the two effects on bacterial adhesion.

4. Conclusions

The results obtained in this work highlight the possibility of developing a uniform anti-adhesive coating on two different bioactive glass compositions (one commercial and the other developed by the authors) using the deposition and plasma treatment of a commercial fluoroalkyl functional water-borne oligosiloxane. The atmospheric plasma technology improves the uniformity and adhesion of the coating and imparts a pillar structure on both glasses, which, together with the exposure of the hydrophobic groups, prevents bacterial adhesion.

The results of in vitro bioactivity demonstrate that there are no significant differences between the two glasses, but above all, that the presence of the coating does not inhibit the bioactivity processes; on the contrary, it seems to speed up the bioactivity kinetics. This effect could be due to the exposure of -NH_2 groups, highlighted by FTIR and zeta potential analysis, which could foster the deposition of HAp. Finally, the evaluation of anti-adhesiveness demonstrated the ability of the plasma-treated coating to decrease the number of viable surface-adherent bacterial colonies. The anti-adhesive effect is certainly imparted by the achieved surface charge and low wettability. Moreover, the topography obtained after plasma treatment may also have played a role in limiting bacterial adhesion.

Therefore, the developed treatment shows promise for conferring anti-adhesive properties to devices for bone regeneration; however, future advances must focus on the evaluation of materials' cytocompatibility.

CRediT authorship contribution statement

Kevin Pontillo: Writing – review & editing, Writing – original draft, Investigation, Formal analysis, Data curation. **Martina Masserano:** Investigation, Formal analysis, Data curation. **Ziba Najmi:** Writing – original draft, Investigation, Formal analysis. **Andrea Cochis:** Writing – original draft, Methodology, Data curation. **Lia Rimondini:** Writing – review & editing, Supervision, Resources, Methodology. **Sara Ferraris:** Writing – original draft, Investigation, Formal analysis. **Katiuscia Costabello:** Writing – review & editing, Supervision, Methodology, Data curation, Conceptualization. **Manuel Lai:** Supervision, Resources, Methodology, Conceptualization. **Enrica Vernè:** Writing – review & editing, Supervision, Methodology, Conceptualization. **Marta Miola:** Writing – review & editing, Writing – original draft, Supervision, Resources, Project administration, Methodology, Funding acquisition, Conceptualization.

Declaration of competing interest

The authors declare that they have no known competing financial interests or personal relationships that could have appeared to influence the work reported in this paper.

Acknowledgments

This study was funded by the European Union's NextGenerationEU under PNRR – M4C2 – AVVISO 3277/2021 – NODES - ECS00000036 – PoC POTENTE.

Data availability

Data will be made available on request.

References

[1] W.M. Dunne, Bacterial adhesion: seen any good biofilms lately? Clin. Microbiol. Rev. 15 (2002) 155–166, https://doi.org/10.1128/CMR.15.2.155-166.2002.
[2] M.H. Muhammad, A.L. Idris, X. Fan, Y. Guo, Y. Yu, X. Jin, J. Qiu, X. Guan, T. Huang, Beyond risk: bacterial biofilms and their regulating approaches, Front. Microbiol. 11 (2020), https://doi.org/10.3389/fmicb.2020.00928.

[3] A. Zhao, J. Sun, Y. Liu, Understanding bacterial biofilms: from definition to treatment strategies, Front. Cell Infect. Microbiol. 13 (2023), https://doi.org/10.3389/fcimb.2023.1137947.
[4] N. Lindfors, J. Geurts, L. Drago, J.J. Arts, V. Juutilainen, P. Hyvönen, A.J. Suda, A. Domenico, S. Artiaco, C. Alizadeh, A. Brychcy, J. Bialecki, C.L. Romanò, Antibacterial bioactive glass S53P4 for chronic bone infections – A multinational study, Adv. Exp. Med. Biol. 971 (2017) 81–92, https://doi.org/10.1007/5584_2016_156.
[5] L. Lazzarini, J.T. Mader, J.H. Calhoun, Osteomyelitis in Long bones, J. Bone Joint Surg. 86 (2004) 2305–2318, https://doi.org/10.2106/00004623-200410000-00028.
[6] X.M. Yang, J.W. Hou, Y. Tian, J.Y. Zhao, Q.Q. Sun, S.B. Zhou, Antibacterial surfaces: strategies and applications, Sci. China Technol. Sci. 65 (2022) 1000–1010, https://doi.org/10.1007/s11431-021-1962-x.
[7] E. Verné, M. Miola, C. Vitale Brovarone, M. Cannas, S. Gatti, G. Fucale, G. Maina, A. Massé, S. Di Nunzio, Surface silver-doping of biocompatible glass to induce antibacterial properties. Part I: massive glass, J. Mater. Sci. Mater. Med. 20 (2009) 733–740, https://doi.org/10.1007/s10856-008-3617-9.
[8] F. Sharifianjazi, M. Sharifianjazi, M. Irandoost, K. Tavamaishvili, M. Mohabatkhah, M. Montazerian, Advances in zinc-containing bioactive glasses: a comprehensive review, J. Funct. Biomater. 15 (2024) 258, https://doi.org/10.3390/jfb15090258.
[9] A. Sayed Abdelgeliel, S. Ferraris, A. Cochis, S. Vitalini, M. Iriti, H. Mohammed, A. Kumar, M. Cazzola, W.M. Salem, E. Verné, S. Spriano, L. Rimondini, Surface functionalization of bioactive glasses with polyphenols from Padina pavonica Algae and In situ reduction of silver ions: physico-chemical characterization and biological response, Coatings 9 (2019) 394, https://doi.org/10.3390/coatings9060394.
[10] M. Miola, E. Bertone, E. Vernè, In situ chemical and physical reduction of copper on bioactive glass surface, Appl. Surf. Sci. 495 (2019) 143559, https://doi.org/10.1016/j.apsusc.2019.143559.
[11] S. Ferraris, M. Miola, A. Cochis, B. Azzimonti, L. Rimondini, E. Prenesti, E. Vernè, In situ reduction of antibacterial silver ions to metallic silver nanoparticles on bioactive glasses functionalized with polyphenols, Appl. Surf. Sci. 396 (2017) 461–470, https://doi.org/10.1016/j.apsusc.2016.10.177.
[12] I. Gonzalo-Juan, F. Xie, M. Becker, D.U. Tulyaganov, E. Ionescu, S. Lauterbach, F. De Angelis Rigotti, A. Fischer, R. Riedel, Synthesis of silver modified bioactive glassy materials with antibacterial properties via facile and low-temperature route, Materials. (Basel) 13 (2020) 5115, https://doi.org/10.3390/ma13225115.
[13] M. Miola, C. Vitale-Brovarone, C. Mattu, E. Verné, Antibiotic loading on bioactive glasses and glass-ceramics: an approach to surface modification, J. Biomater. Appl. 28 (2013) 308–319, https://doi.org/10.1177/0885328212447665.
[14] K. Zheng, M. Lu, Y. Liu, Q. Chen, N. Taccardi, N. Hüser, A.R. Boccaccini, Monodispersed lysozyme-functionalized bioactive glass nanoparticles with antibacterial and anticancer activities, Biomed. Mater. 11 (2016) 035012, https://doi.org/10.1088/1748-6041/11/3/035012.
[15] S. Shaikh, D. Singh, M. Subramanian, S. Kedia, A.K. Singh, K. Singh, N. Gupta, S. Sinha, Femtosecond laser induced surface modification for prevention of bacterial adhesion on 45S5 bioactive glass, J. Non. Cryst. Solids. 482 (2018) 63–72, https://doi.org/10.1016/j.jnoncrysol.2017.12.019.
[16] C. Pontremoli, I. Izquierdo-Barba, G. Montalbano, M. Vallet-Regí, C. Vitale-Brovarone, S. Fiorilli, Strontium-releasing mesoporous bioactive glasses with anti-adhesive zwitterionic surface as advanced biomaterials for bone tissue regeneration, J. Colloid. Interface Sci. 563 (2020) 92–103, https://doi.org/10.1016/j.jcis.2019.12.047.
[17] M. Miola, K. Pontillo, K. Costabello, M. Lai, S. Ferraris, Z. Najmi, A. Cochis, L. Rimondini, E. Vernè, Surface modifications of inert and bioactive glasses with plasma-deposited polymer coatings to impart antiadhesive properties, Surf. Interfaces. 64 (2025) 106346, https://doi.org/10.1016/j.surfin.2025.106346.
[18] A. Nikiforov, C. Ma, A. Choukourov, F. Palumbo, Plasma technology in antimicrobial surface engineering, J. Appl. Phys. 131 (2022) 011102, https://doi.org/10.1063/5.0066724.
[19] M. Guo, F. Meng, G. Li, J. Luo, X. Xia, Effective antibacterial glass Fiber membrane prepared by plasma- enhanced chemical grafting, ACS. Omega 4 (2019) 16591–16596, https://doi.org/10.1021/acsomega.9b02403.
[20] C. Tran, M. Yasir, D. Dutta, N. Eswaramoorthy, N. Suchowerska, M. Willcox, D. R. Mckenzie, Single step plasma process for covalent binding of antimicrobial peptides on catheters to suppress bacterial adhesion, ACS. Appl. Bio Mater. 2 (2019) 5216–6028, https://doi.org/10.1021/acsabm.9b00776.
[21] K.S. Siow, A.S. Abdul Rahman, P.Y. Ng, B.Y. Majlis, Sulfur and nitrogen containing plasma polymers reduces bacterial attachment and growth, Mater. Sci. Eng. C (2020) 107, https://doi.org/10.1016/j.msec.2019.110225.
[22] M. Miola, G. Fucale, G. Maina, E. Verné, Antibacterial and bioactive composite bone cements containing surface silver-doped glass particles Antibacterial and bioactive composite bone cements containing surface silver-doped glass particles, Biomed. Mater. 10 (2015), https://doi.org/10.1088/1748-6041/10/5/055014.
[23] S. Fagerlund, J. Massera, N. Moritz, L. Hupa, M. Hupa, Phase composition and in vitro bioactivity of porous implants made of bioactive glass S53P4, Acta Biomater. 8 (2012) 2331–2339, https://doi.org/10.1016/j.actbio.2012.03.011.
[24] T. Kokubo, H. Takadama, How useful is SBF in predicting in vivo bone bioactivity? Biomaterials 27 (2006) 2907–2915, https://doi.org/10.1016/j.biomaterials.2006.01.017.
[25] Z. Yu, Z. Wang, Y. Chen, Y. Wang, L. Tang, Y. Xi, K. Lai, Q. Zhang, S. Li, D. Xu, A. Tian, M. Wu, Y. Wang, G. Yang, C. Gao, T. Huang, Programmed surface platform orchestrates anti-bacterial ability and time-sequential bone healing for implant-associated infection, Biomaterials 313 (2025), https://doi.org/10.1016/j.biomaterials.2024.122772.
[26] Preparation of routine Media and reagents used in antimicrobial susceptibility testing, Clinical Microbiology Procedures Handbook, ASM Press, 2016, https://doi.org/10.1128/9781555818814.ch5.20.1, 5.20.1.1-5.20.3.10.
[27] M.D. Hoffman, L.I. Zucker, P.J.B. Brown, D.T. Kysela, Y.V. Brun, S.C. Jacobson, Timescales and frequencies of reversible and irreversible adhesion events of single bacterial cells, Anal. Chem. 87 (2015) 12032–12039, https://doi.org/10.1021/acs.analchem.5b02087.
[28] M. Lallukka, M. Miola, Z. Najmi, A. Cochis, S. Spriano, L. Rimondini, E. Verné, Cu-doped bioactive glass with enhanced in vitro bioactivity and antibacterial properties, Ceram. Int. 50 (2024) 5091–5103, https://doi.org/10.1016/j.ceramint.2023.11.253.
[29] D.A. Bellido-Aguilar, S. Zheng, X. Zhan, Y. Huang, X. Zhao, X. Zeng, P. K. Pallathadka, Q. Zhang, Z. Chen, Effect of a fluoroalkyl-functional curing agent on the wettability, thermal and mechanical properties of hydrophobic biobased epoxy coatings, Surf. Coat. Technol. 362 (2019) 274–281, https://doi.org/10.1016/j.surfcoat.2019.02.006.
[30] S. Cai, C. Wu, W. Yang, W. Liang, H. Yu, L. Liu, Recent advance in surface modification for regulating cell adhesion and behaviors, Nanotechnol. Rev. 9 (2020) 971–989, https://doi.org/10.1515/ntrev-2020-0076.
[31] W. J, Y. M, T. S, H. M, K. E, L. B, O. Y, Adhesion of mouse fibroblasts on hexamethyldisiloxane surfaces with wide range of wettability, J. Biomed. Mater. Res. B Appl. Biomater. 81 (2007) 66–75, https://doi.org/10.1002/jbmb.
[32] I. Georgakopoulos-Soares, E.L. Papazoglou, P. Karmiris-Obratański, N.E. Karkalos, A.P. Markopoulos, Surface antibacterial properties enhanced through engineered textures and surface roughness: a review, Colloids. Surf. B Biointerfaces. 231 (2023), https://doi.org/10.1016/j.colsurfb.2023.113584.
[33] M. Mu, S. Liu, W. DeFlorio, L. Hao, X. Wang, K.S. Salazar, M. Taylor, A. Castillo, L. Cisneros-Zevallos, J.K. Oh, Y. Min, M. Akbulut, Influence of surface roughness, nanostructure, and wetting on bacterial adhesion, Langmuir. 39 (2023) 5426–5439, https://doi.org/10.1021/acs.langmuir.3c00091.
[34] A. Uneputty, A. Dávila-Lezama, D. Garibo, A. Oknianska, N. Bogdanchikova, J. F. Hernández-Sánchez, A. Susarrey-Arce, Strategies applied to modify structured and smooth surfaces: a step closer to reduce bacterial adhesion and biofilm formation, Colloid. Interface Sci. Commun. 46 (2022), https://doi.org/10.1016/j.colcom.2021.100560.
[35] E.E. Mann, D. Manna, M.R. Mettetal, R.M. May, E.M. Dannemiller, K.K. Chung, A. B. Brennan, S.T. Reddy, Surface micropattern limits bacterial contamination, Antimicrob. Resist. Infect. Control 3 (2014), https://doi.org/10.1186/2047-2994-3-28.
[36] S. Ferraris, S. Yamaguchi, N. Barbani, M. Cazzola, C. Cristallini, M. Miola, E. Vernè, S. Spriano, Bioactive materials: in vitro investigation of different mechanisms of hydroxyapatite precipitation, Acta Biomater. (2019) 0–38, https://doi.org/10.1016/j.actbio.2019.11.024.
[37] M. Kosmulski, pH-dependent surface charging and points of zero charge. IV. Update and new approach, J. Colloid. Interface Sci. 337 (2009) 439–448, https://doi.org/10.1016/j.jcis.2009.04.072.
[38] I. Hirata, M. Akamatsu, E. Fujii, S. Poolthong, M. Okazaki, Chemical analyses of hydroxyapatite formation on SAM surfaces modified with COOH, NH2, CH3, and OH functions, Dent. Mater. J. 29 (2010) 438–445, https://doi.org/10.4012/dmj.2010-017.
[39] P. Speziale, G. Pietrocola, T.J. Foster, J.A. Geoghegan, Protein-based biofilm matrices in staphylococci, Front. Cell Infect. Microbiol. 4 (2014), https://doi.org/10.3389/fcimb.2014.00171.
[40] Q. Peng, X. Tang, W. Dong, N. Sun, W. Yuan, A review of biofilm formation of Staphylococcus aureus and its regulation mechanism, Antibiotics 12 (2023), https://doi.org/10.3390/antibiotics12010012.
[41] E. Sharifikolouei, Z. Najmi, A. Cochis, A.C. Scalia, M. Aliabadi, S. Perero, L. Rimondini, Generation of cytocompatible superhydrophobic Zr–Cu–Ag metallic glass coatings with antifouling properties for medical textiles, Mater. Today Bio 12 (2021) 100148, https://doi.org/10.1016/j.mtbio.2021.100148.
[42] D. Wang, P. Gao, M. Zheng, Z. Duan, D. Wang, D. Ding, F. Xia, Mechanically durable plant-based composite surface towards enhanced antifouling properties, J. Colloid. Interface Sci. 679 (2025) 457–466, https://doi.org/10.1016/j.jcis.2024.10.106.
[43] J.D.C. Tardelli, L.B. Otani, R.L. Batalha, F. Alves, M.A. Pereira-da-Siva, V. S. Bagnato, P. Gargarella, C. Bolfarini, A.C. dos Reis, Atomic Interaction S. aureus/machined and additive manufacturing Ti-6Al-4V and Ti-35Nb-7Zr-5Ta disks for dental implants, J. Biomed. Mater. Res. B Appl. Biomater. (2024) 112, https://doi.org/10.1002/jbm.b.35508.